Few-Mode Based Beam Shaping for Multi-User Indoor Optical Wireless Communications With Time-Slot Coding

Jianghao Li [ID], Christina Lim [ID], *Senior Member, IEEE*, and Ampalavanapillai Nirmalathas [ID], *Senior Member, IEEE*

Abstract—We propose a novel indoor optical wireless communications (OWC) system using few-mode based beam shaping integrating time-slot coding (TSC) scheme to serve multiple users simultaneously. We simulated an indoor OWC system incorporating single-sideband (SSB) 16 quadrature amplitude modulation (16-QAM) modulated signals in a multi-user environment employing few-mode based beam shaping with single-photodetector (PD) and multi-PD reception with maximum ratio combining (MRC), respectively. The results show that for both single-PD and multi-PD receptions, the bit-error-rate (BER) performance can be significantly improved at different positions within the cell and the size of the effective coverage (BER$<3.8 \times 10^{-3}$) can be increased by 4 times by employing few-mode based beam shaping scheme at 1:1.79 power ratio between LP_{01} mode and LP_{11} mode, compared to conventional OWC systems without few-mode based beam shaping scheme. In addition, the system tolerance to signal overlapping can also be enhanced with the proposed few-mode based beam shaping. The optimal power ratios of LP_{01} mode and LP_{11} mode when achieving the maximum effective coverage under 7% and 20% HD-FEC thresholds for single-PD and multi-PD reception have also been investigated. Furthermore, the tolerance to the interval delay with 0.23 and 0.28 symbols can be achieved in single-PD and multi-PD reception, respectively.

Index Terms—Optical wireless communication, multiple access, beam shape, Kramers-Kronig receiver, wireless personal area networks.

I. INTRODUCTION

INDOOR optical wireless communications (OWC) have attracted an increased attention in recent years as a promising technology for the provision of ultra-wideband communications [1]. In previous research, indoor OWC with multiple spatial channels and a total data rate exceeding 250 Gb/s for multiple user access has been experimentally demonstrated [2]. Besides, high-speed OWC with single spatial channel for multiple user scenario has also been widely investigated [3]. In previous studies, different techniques such as time-division multiple access (TDMA), subcarrier or frequency-division multiple access (FDMA), and code-division multiple access (CDMA) [4], [5] have been proposed and demonstrated in OWC systems to cater for multi-user access. In recent time, time-slot coding (TSC) has been proposed to provide multi-access for indoor OWC system [6], which offers the advantages of a simpler implementation coupled with better immunity to the interference among the users. However, a key problem for multi-user OWC with the Gaussian-shaped beam profile often associated with the lasers used today with power distribution across the beam being not uniform. This results in performance experienced by different users to vary remarkably depending on their positions because of the non-uniform received signal power distribution within the same cell [7]. As the user moves away from the beam center, the performance declines significantly because the received power decreases with the Gaussian-shaped power distribution. Therefore, beam shaping techniques are highly needed for providing enhanced performance in an OWC multi-user environment.

Many techniques have been proposed and demonstrated to transform the Gaussian-shaped beam into other beams with different power distribution. In [8] and [9], the authors have achieved a flattop beam using refractive and diffractive techniques respectively. In addition, indirect beam shaping which first splits the input beam into many beamlets and then use beam homogenizers or integrators to superpose them into a beam with new power distribution has also been proposed and experimentally demonstrated [10]. However, these two techniques require many bulky optical components which are very difficult to be integrated in on-chip systems in addition to significant power consumption during the refraction or diffraction process. In [11], a uniform intensity beam is obtained by coherently superposing two modes from the same long period grating (LPG). In [12] and [13], vortex beams with various intensity distribution were obtained by combining a Laguerre-Gaussian (LG)-shaped and a Gaussian-shaped vortex beams. However, both the uniform beam generated by LPG and the combined vortex beams can be only achieved at a specific distance from the transmitter or on the focal plane, which makes them not suitable for practical OWC systems due their limited transmission distance and system flexibility. Another effective way to improve the system resistance to the performance degradation caused by power fading is employing multi-mode or few-mode based spatial diversity reception which can provide multiple spatial super-channels to resist power fading simultaneously [14]. By superposing different spatial modes in few-mode fiber (FMF), a uniform optical

beam has been achieved in [15]. We have recently adopted this scheme to propose and experimentally demonstrate a uniform beam shaping by the superposition of different spatial linear-polarized modes (few-mode) for indoor point-to-point OWC systems [7], [16]. High-quality uniform beam has been realized and 10 Gb/s data with on-off keying (OOK) modulation format was transmitted over the uniform beam with error-free transmission. Nevertheless, few-mode based beam shaping for multi-user transmission in OWC has not been studied and investigated.

In this paper, we proposed few-mode based beam shaping for multi-user transmission with time-slot coding for indoor OWC environment, for the first time, to the best of our knowledge. In addition, we simulated different receiver configurations using both a single photodetector (PD) and multiple PDs with maximum ratio combining (MRC) scheme respectively. Here, the numerical simulations are performed to thoroughly understand the characteristics of the shaped beam and how it impacts the user performance in a multi-user environment. The bit-error-rate (BER) performance under different signal overlapping ratios and power ratios of the fundamental (LP_{01}) and the 2nd-order (LP_{11}) modes is investigated and discussed. The results show that for both single-PD and multi-PD receptions, the user BER performance is improved at different positions with enhanced performance within the cell and the size of the effective coverage (BER$<3.8\times10^{-3}$) can be increased by 4 times with the proposed beam shaping scheme when the power ratio of LP_{01} mode and LP_{11} mode is about 1:1.79, compared to the conventional OWC systems without the proposed beam shaping. In addition, for single-PD and multi-PD receiver configurations, the optimal power ratios of LP_{01} mode and LP_{11} mode when achieving the maximum effective coverage under 7% and 20% hard-decision forward error correction (HD-FEC) thresholds with gross data rate of 10 Gb/s with 4 served users have been discussed. More importantly, the tolerance to signal overlapping caused by imperfect timing of time-slot coding can also be enhanced with the proposed few-mode based beam shaping and the maximum tolerance of 0.23 and 0.28 symbols to the interval delay caused by different mode delay can be obtained in single-PD and multi-PD reception, respectively.

The rest of this paper is organized as follows: Section II presents the theoretical models of few-mode based beam shaping and time-slot coding. Section III illustrates the simulation setup and results. Section IV concludes the paper.

II. PRINCIPLES OF FEW-MODE BASED BEAM SHAPING

The basic idea of few-mode based beam shaping is by superposing a Gaussian-shaped fundamental beam and a donut-shaped LP_{11} beam with different power ratio to obtain different shaped beams, under the assumption that the refractive index of the few-mode fiber is step-indexed. According to the theory of light propagating within an optical fiber under the regime governed by Maxwell equations, the electromagnetic field distribution of LP_{01} and LP_{11} modes at the end facet can be expressed as [17]

$$E_{01} = E\frac{J_1(u_{01}r/a)}{J_1(u_{01})}, \qquad (1)$$

$$E_{11} = E\frac{J_1(u_{11}r/a)}{J_1(u_{11})}, \qquad (2)$$

respectively, where E is the maximum value of the electrical field at the interface between cladding and core. a is the core radius of the FMF and r depicts the radial coordinates with $r<a$. J_1 depicts the first-order Bessel function and u_{01} and u_{11} represent the transverse phase parameter of LP_{01} and LP_{11} mode respectively. LP_{11} mode can be treated as a linear combination of different vector modes including TE_{01}, TM_{01}, HE_{21a}, and HE_{21b}. Different LP_{11} modes with various power distribution and polarization can be obtained by combining TE_{01} and TM_{01} modes with HE_{21} modes with different phases, which is defined as a cluster of LP_{11} modes. Therefore, the transverse electromagnetic field of LP_{11} mode cluster can be expressed as

$$E_{11}(r,\varphi) = E\frac{J_1(u_{11}r/a)}{J_1(u_{11})} * \left\{ \begin{array}{c} \overrightarrow{x}\sin\varphi \\ \overrightarrow{x}\cos\varphi \\ \overrightarrow{y}\sin\varphi \\ \overrightarrow{y}\cos\varphi \end{array} \right\} = \left\{ \begin{array}{c} LP_{11bx} \\ LP_{11ax} \\ LP_{11by} \\ LP_{11ay} \end{array} \right\}, \qquad (3)$$

where φ denotes the azimuthal coordinate. $\overrightarrow{x}$ and $\overrightarrow{y}$ represent the horizontal and vertical polarization direction, respectively. The key step for few-mode based beam shaping is to generate a donut-shaped beam by adjusting the birefringence in FMF which can be expressed as [18]

$$E_{donut} = b_1\left(LP_{11ax} + LP_{11bx}e^{i\phi}\right)\overrightarrow{x}$$
$$+ b_2e^{i\psi}\left(LP_{11ay} + LP_{11by}e^{i\phi}\right)\overrightarrow{y} \quad \phi = (2n+1)\pi/2 \quad (4)$$

where ψ represents the angle difference between vertical (y) coordinate and the current polarization and ϕ denotes the phase difference between LP_{11a} and LP_{11b} within the same polarization. Substituting equations (1), (2) and (3) into (4), the electromagnetic field of the donut-shaped beam can be rewritten as

$$E_{donut} = (b_1 + b_2)(\cos\varphi + e^{i\phi}\sin\varphi)E\frac{J_1(u_{11}r/a)}{J_1(u_{11})}. \quad (5)$$

The final output beam can be obtained by superposing the donut-shaped LP_{11} mode and the fundamental beam incoherently, which can be expressed as

$$E_t = c_1E_{01} + c_2E_{donut} \qquad (6)$$

where c_1 and c_2 denote the power coefficients of LP_{01} beam and donut-shaped beam. Different shapes of the combined beam can be obtained by changing the power coefficients. Substituting equations (1) and (5) into (6), the electromagnetic field of the combined beam can be written as

$$E_t = c_1E\frac{J_1(u_{01}r/a)}{J_1(u_{01})}$$

$$+ (b_1 + b_2)c_2(\cos\varphi + e^{i\phi}\sin\varphi)E\frac{J_1(u_{11}r/a)}{J_1(u_{11})}$$

$$= m_1E\frac{J_1(u_{01}r/a)}{J_1(u_{01})}$$

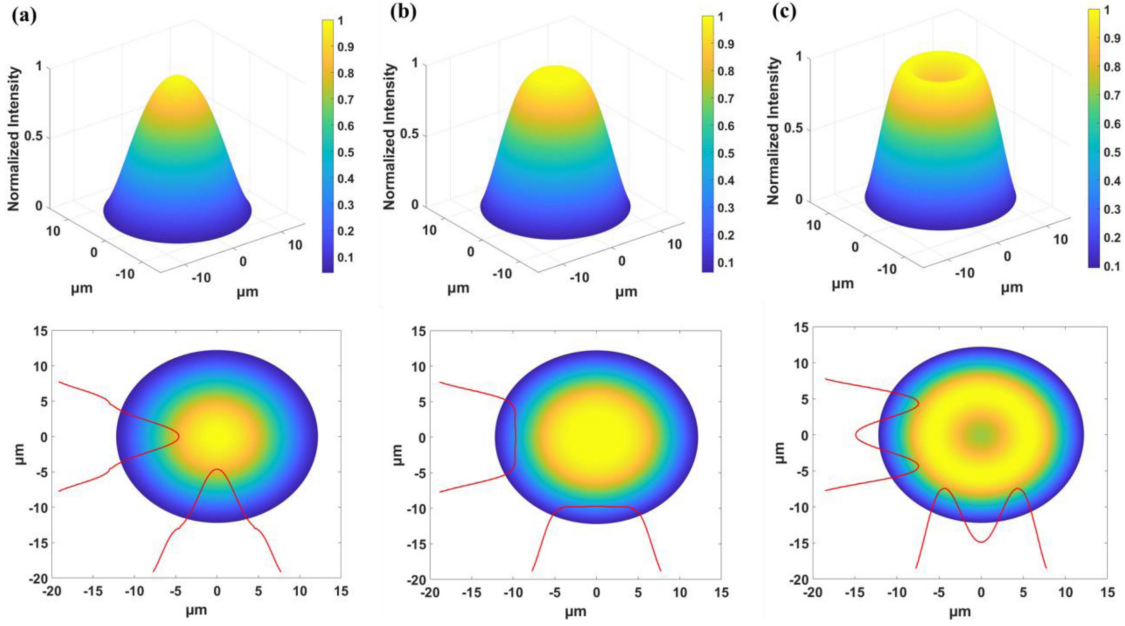$$+ m_2(\cos\varphi + e^{i\phi}\sin\varphi)E\frac{J_1(u_{11}r/a)}{J_1(u_{11})} \qquad (7)$$

Fig. 1. 1D, 2D, and 3D profiles of the simulated intensity distribution of the combined beams with power ratio between LP_{01} mode and LP_{11} mode of (a) 1:0.86, (b) 1:1.79, and (c) 1:4.57.

where $m_1 = c_1$ and $m_2 = (b_1 + b_2)c_2$. In order to explore the relationship of the power between the combined signal and the input LP_{01} and LP_{11} modes, here we define the power ratio of LP_{01} and LP_{11} mode as $1/\gamma$, where γ can be expressed as

$$\gamma = \frac{m_2^2}{m_1^2} \cdot \left| \frac{J_1(u_{11}r/a) J_1(u_{01})}{J_1(u_{01}r/a) J_1(u_{11})} \right|^2 \tag{8}$$

The simulated intensity distribution of the combined beam using few-mode based beam shaping at the output of the beam splitter is shown in Fig. 1. In order to avoid any mode interference between LP_{01} and LP_{11} mode, we generate LP_{01} mode and LP_{11} mode from different light source with the wavelength of 1549nm and 1551nm respectively. Figs 1(a)–(c) show the power distribution of the combined beam for the power ratios of the LP_{01} mode and the donut-shaped LP_{11} mode of 1:0.86, 1:79, and 1:4.57, respectively. It can be found that the combined beam with a concave center is being filled gradually to a flattop beam as the power ratio increases to 1:1.79. In addition, when the power ratio exceeds 1:1.79, the beam profile will convert into a Gaussian shape.

III. SIMULATIONS AND RESULTS

A. Simulation Setup

We conduct numerical simulations to overcome the practical device limitations in multi-user scenario implementation that requires many components for proper experimental evaluation. Fig. 2(a) shows the simulation set-up of the few-mode based beam shaping for multi-user transmission with time-slot coding in an indoor OWC environment. For simplicity of the illustration, only one user is shown in Fig. 2. The other users have the same configuration as the user shown in Fig. 2 and are located at different positions with distance (*d*) away from the beam

center. As described in [19], a pseudo-random binary sequence (PRBS) with the length of $2^{15}-1$ is first split into *k* copies of sequence for *k* served users, which is shown as Fig. 3(a). After baseband modulation, to avoid signals of different users becoming overlapped in the frequency domain during the down-sampling process which is implemented in the final digital signal processing (DSP) stage, each user was allocated to different frequency locations. This helps with down-sampling and avoids issues in the data recovery at the receiver. In the simulation, the frequency allocation is achieved by shifting the frequencies of different users. After frequency shifting, U_1 is assigned to the highest frequency while U_k is assigned to the lowest frequency. In addition, each user shares $1/k$ times the total bandwidth of the system $k\omega$. Therefore, U_1 is assigned to the frequency location of $((k-1)\omega\ k\omega]$ while U_k is assigned to $(0\ \omega]$. In time domain, each sequence is multiplied with a dedicated time-slot code which consists of *k*-bit binary values (0 and 1). As illustrated in Fig. 3(b), each TSC has a bit '1' at a unique bit location and only one user can be served at the time slot with bit '1'. Next, the time-slot coded sequences are summed up with ideal code alignment and each non-overlapped time slot is assigned with a single served user to avoid interference which is shown in Fig. 3(c), After that, the resulting TSC data is sent to an arbitrary waveform generator (AWG) to drive two IQ modulators (Mods) to obtain 16 quadrature amplitude modulation (16-QAM) for-matted optical signals from two external cavity lasers (ECLs) with wavelengths of 1549nm and 1551nm, respectively. Here two different wavelengths are used to eliminate the coherent interference at the receiver that may arise in the beam shaping. To construct single-sideband (SSB) signals and for data recovery with Kramers-Kronig (K-K) reception, we insert a carrier at the lower frequency of the modulated signals with the carrier-to-signal power ratio (CSPR) of 6 dB. The ideal (without insertion
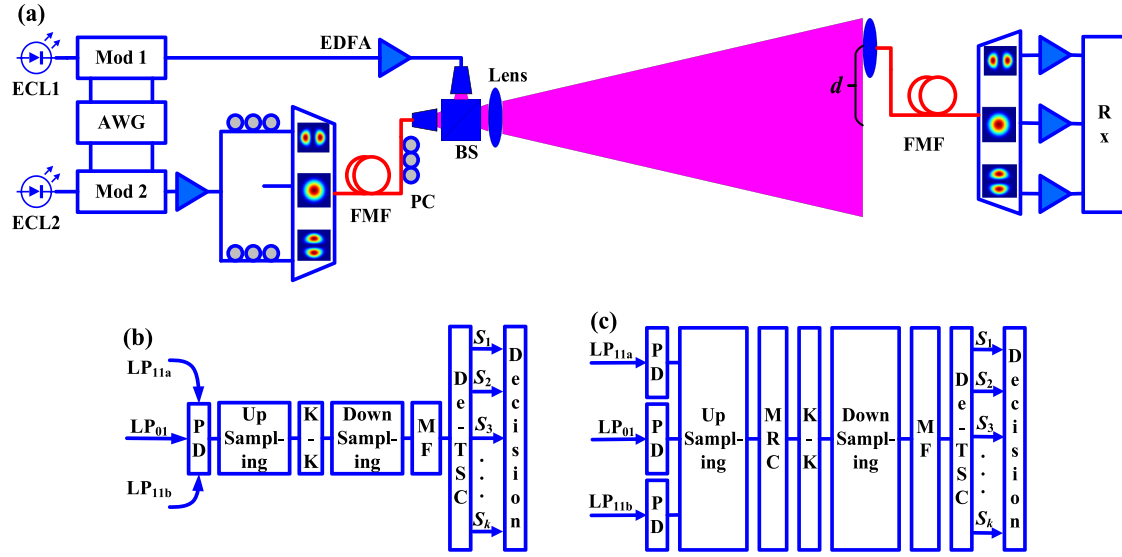
Fig. 2.   (a) Simulation setup. (b) DSP of single-PD reception. (c) DSP of multi-PD reception.
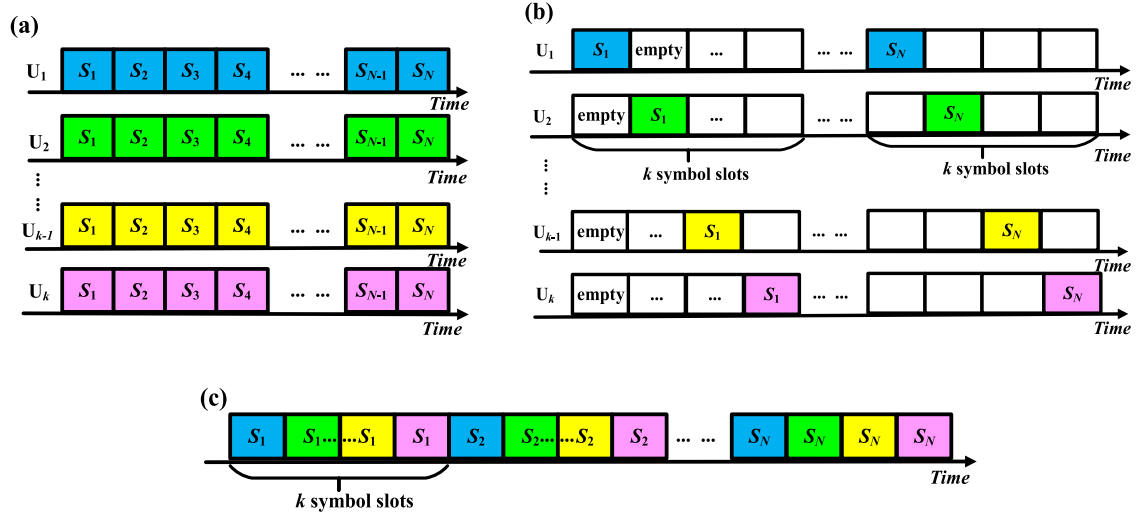

Fig. 3.   (a) Original data for k users [19]. (b) TSC coded data sequences for each user [19]. (c) Summed data sequences [19].

loss and mode crosstalk) mode selective multiplexer (MUX) is simulated according to equation (2) and (3) to provide LP_{11a} and LP_{11b} modes. LP_{11a} and LP_{11b} modes can be degenerated into a donut-shaped beam by introducing birefringence in FMF by adjusting the polarization controls (PCs). The polarization of the LP_{11a} and LP_{11b} modes needs to be adjusted precisely with PCs to obtain the donut beam according to equation (4) and (5). The polarization misalignment can result in non-uniform power distribution along the donut-shaped LP_{11} beam or the failure to obtain the donut beam. Finally, the LP_{01} beam and the donut-shaped beam are superposed using a 50:50 beam splitter (BS). Here the BS is employed to make sure that the transmitted LP_{01} and donut beams can be superposed concentrically. Different shapes of the superposed optical beam can be obtained by adjusting the power ratio of LP_{01} and the donut-shaped beam. The transmission channel is modeled as

an indoor optical wireless link with an expanded beam with a diameter about 46 cm for multi-user link. The transmission distance is set as 2 m and the divergence angles of LP_{01} and LP_{11} mode are set as 7.7° and 13.4° respectively. The total transmitted optical power is set to 6 dBm which satisfies the regulation of the eye and skin safety [20]. Since the typical propagation path loss for indoor optical wireless communications in bright environment condition is about 0.2–3 dB/km [21], it is negligible for 2 meters indoor optical wireless transmission in our simulation.

At the receiver side, the optical signals are collected by a lens with diameter of 3 cm and coupled into the FMF. The coupling efficiency of the lens is modelled as [22]

$$\eta = \frac{m+1}{2\pi}\cos^{m}(\theta), \qquad (9)$$

where θ is the divergence angle and m is the Lambert's mode number which can be expressed as [22]

$$m = \frac{-\ln 2}{\ln \left(\cos \Theta_{1/2}\right)}, \qquad (10)$$

where $\Theta_{1/2}$ is the semi-angle at half power of the light source. The ideal (without insertion loss and mode crosstalk) mode selective de-multiplexer (De-MUX) is modeled to convert the few-mode signals into LP_{01} mode signals. Additive white Gaussian noise (AWGN) is added to the 3 branches of signals to emulate different optical signal-to-noise ratios (OSNRs). Here we assume that the noise is dominated by the background light and the thermal and quantum noise from the PDs. It is noted that OSNR takes the power of both carrier and the modulated signals into consideration in the system. After being amplified by erbium doped fiber amplifiers (EDFAs), the received optical signals are converted into photocurrents by square law detection. The converted photocurrents are first up-sampled to 4 samples per symbol by a digital storage oscilloscope (DSO) for analog-to-digital conversion and off-line DSP. The DSP of a single-PD reception and multi-PD reception with MRC is depicted as Fig. 2(b) and (c) respectively. In the single-PD reception, the optical signals from different modes are coupled into the same fiber and detected by a single PD and sampled by a single channel of the DSO. On the other hand, in multi-PD reception, the three-branch optical signals are received using the respective PDs and sampled by different channels of the DSO. Then the sampled signals are combined with MRC algorithm. The weight coefficients of each branch in the MRC algorithm are selected as $\alpha_i = P_i/P$, where P_i is the power of the i-th down-sampled photocurrent and can be expressed as $P_i = \|S_i\|^2$, where S_i is the signal of the i-th branch and P is the sum of the power of the 3 branches of signals. Next, the K-K relation is operated for phase and optical field recovery. The latter stage consists of a down sampling process that reduces the samples to 2 samples per symbol in frequency domain. After that, we decode the TSC (De-TSC) signals by multiplying the respective TSC to serve different users after the matched filter (MF) and data splitting. In contrast to the existing TSC scheme as described in [19], here we set the amplitude and phase recovery stage ahead of the data splitting and De-TSC to eliminate the impact of code misalignment on the amplitude and phase recovery. Finally, the BER of the recovered signals of each user are calculated subject to hard decision.

B. Results and Discussion

Fig. 4 compares the BER performance of the OWC system with few-mode based beam shaping with single-PD and multi-PD receptions and conventional OWC without few-mode based beam shaping (single-mode) at different distance away from the beam center. In the simulation, the power ratio of the LP_{01} mode and LP_{11} mode is set as 1:1.79. The gross bit rate is 10 Gb/s with 16-QAM modulation. The 4 users (U_1-U_4) are uniformly distributed on a circle at a fixed distance away from the beam center. It is noted that the conventional single-mode
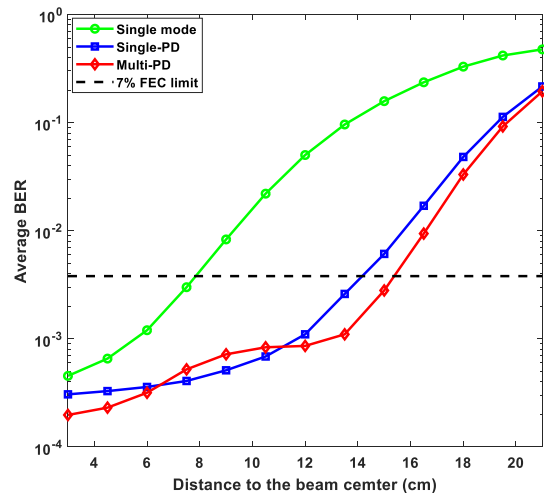

Fig. 4. BER performance comparison of the OWC system with few-mode based beam shaping with single-PD and multi-PD receptions and conventional OWC with single-mode transmission.

system has the same transmitting power as our proposed system using few-mode based beam shaping. The reference BER level is 7% HD-FEC threshold of 3.8×10^{-3} [23]. Compared with conventional single-mode OWC, the BER performance has been improved significantly when using few-mode based beam shaping with both single-PD and multi-PD receptions. The radius of the effective coverage (BER$<3.8\times10^{-3}$) when using single-mode transmission is only about 7.5 cm while the radius of the effective coverage of the system with few-mode based beam shaping with single-PD and multi-PD reception is $\sim$14 cm and 15 cm, respectively. The area of the effective coverage has been improved about 4 times by employing the few-mode based beam shaping. Besides, we can see that multi-PD reception outperforms single-PD reception when the users are located near the beam center (at distance less than 6 cm) and at the boundary of the cell (at distance more than 11 cm), however this is reversed when the users are located at a distance of 6–11 cm away from the beam center. This is due to the MRC algorithm in multi-PD reception. To clarify, when the distance is less than 6 cm, the LP_{01} channel dominates the performance resulting in multi-PD reception producing better performance compared to the case of single-PD reception. Similarly, when the distance is more than 11 cm, the LP_{11} channel dominates the performance also resulting in better performance in multi-PD reception. However, when the distance is 6–11 cm, there is little difference between LP_{01} and LP_{11} channels resulting in little advantage in using multi-PD reception. Despite the advantage of multi-PD reception, more thermal and quantum noise is induced in multi-PD reception as more PDs are employed.

In order to investigate the performance of each single served user, we illustrates the BER performance of all users at different locations (uniformly distributed on a circle at a fixed distance away from the beam center) when the power ratio of LP_{01} and LP_{11} is 1:1.79 which is shown as Fig. 5. For ease of illustration, here we only investigate the BER performance of the served users when employing single-PD reception as it can achieve
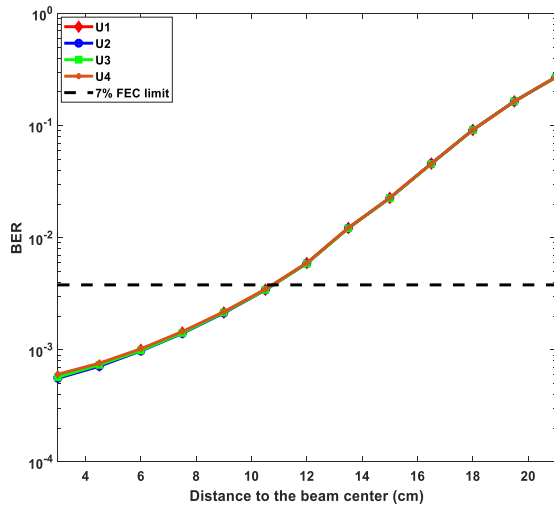
Fig. 5.   BER performance of single-PD reception for each single user.

Fig. 7.   Average BER performance of single-PD reception with different number of served users when the gross data rate is 10 Gb/s.
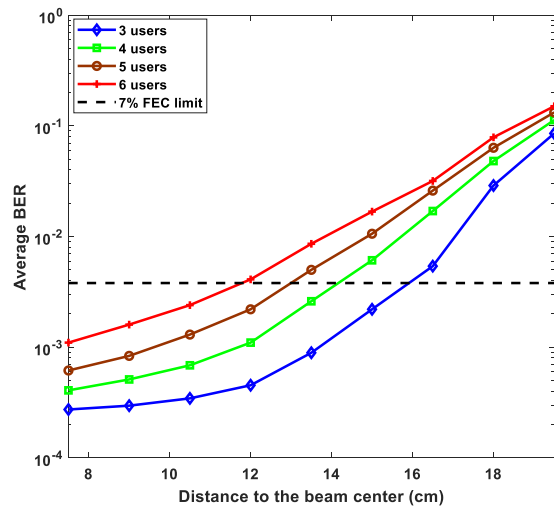

Fig. 6.   Average BER performance of single-PD reception with different number of served users when the data rate is 2.5 Gb/s for each user.

similar performance as the multi-PD reception as shown in Fig. 4 and moreover it possesses the advantages of simple construction and low cost as compared with multi-PD reception. In addition, we select a higher CSPR value of 7.5 dB while the total transmitted optical power remains unchanged in the simulation to avoid some possible side effects such as signal-signal beat interference (SSBI) [24] to the performance of the served users. As shown, similar performance with little difference can be achieved among all the users. This result can be attributed to the reason that all users are treated fairly in TSC scheme, which results in minimal difference in performance amongst them.

In order to investigate the impact of the number of served users in the system, we present the BER performance of single-PD reception with 3-6 users for a power ratio $LP_{01}:LP_{11}$ of 1:1.79. The data rate of each user is 2.5 Gb/s. As illustrated in Fig. 6, it is obvious that the BER increases with the number of the served users in the system. This happens because the gross data rate increases with the number of the served users which results in
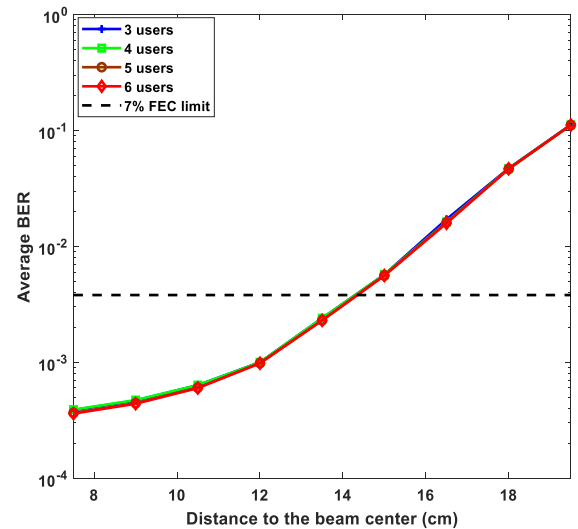
the increased of noise level with the electrical bandwidth of the signals. In another word, since only one user can be served at one single time slot, the required time slots increase with an increase in the number of served users. Therefore, the duration of each time slot decreases with the number of the served users when the total duration of the whole block of all time slots is fixed. The actual data rate of each user will need to increase due to the decrease of the duration of the single time slot, also resulting in the increase of noise level with the electrical bandwidth of the signals. As a consequence, there is a trade-off between the number of the served users and effective coverage (when BER $\leq 3.8 \times 10^{-3}$). Nevertheless, when the gross transmission data rate is maintained at 10 Gb/s, the average BER performance of single-PD and multi-PD reception does not vary with the number of served users (3 to 6) as shown in Fig. 7. However, the data rate per user decreases with the number of the served users. Therefore, there is also a trade-off between the total number of served users and the achievable data rate per user. Besides, it can be observed from both Fig. 6 and Fig. 7 that the average BER performance increases when the user moves away from the beam center regardless of the number of the served users. This happens because the received power of the carrier and the signals decreases when the users move further away from the beam center while the noise does not vary much.

Though the inter-user interference (IUI) in multi-user transmission can be eliminated by employing non-overlapped TSC scheme, in practical scenarios, the signal overlapping caused by imperfect timing during the TSC generation is almost inevitable. In order to evaluate the impact of signal overlapping of TSC as described in [19] to the system performance, we illustrates the calculated BER performance of neighboring users plotted as a function of the overlapping ratio for the OWC system with few-mode based beam shaping incorporating single-PD or multi-PD receptions which is shown as Fig. 8(a) and also shown is the result for conventional OWC with single-mode reception. For ease of analysis, only two users are taken into account in the
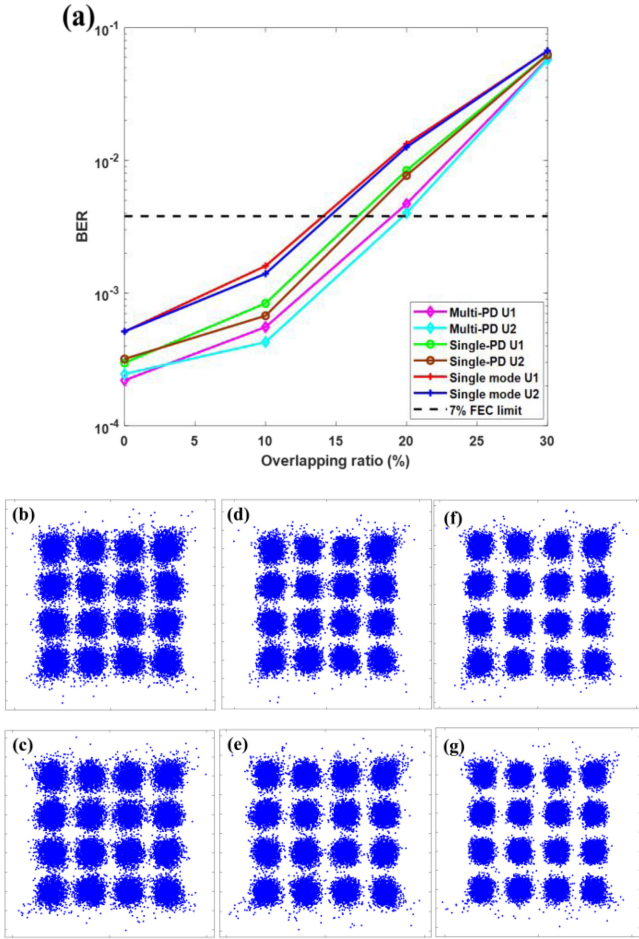
Fig. 8. (a) BER performance versus overlapping ratio. (b), (d), (f) Constellations of received signals of U1 with single-mode, single-PD and multi-PD reception at signal overlapping ratio of 10%. (c), (e), (g) Constellations of received signals of U2 with single-mode, single-PD and multi-PD reception at signal overlapping ratio of 10%.

Fig. 9. Average BER performance of (a) multi-PD reception and (b) single-PD reception with different power ratios LP_{01} and LP_{11} modes.

simulation of the code overlapping tolerance investigation. The distance to the beam center is set as 4.5 cm. It can be seen that the overlapping tolerance of the single-mode, single-PD and multi-PD receptions is ∼13%, 16%, and 20%, respectively, when the error-free threshold is set as the 7% FEC limit. Therefore, we can conclude that the signal overlapping tolerance can be improved by using the proposed few-mode based beam shaping. It is also observed that multi-PD and single-PD receptions performed better than for single-mode transmission when the overlapping ratio is 10% as illustrated from the constellation diagrams in Figs. 8(b)–(g). The reason for this is that the system OSNR can be improved by few-mode based beam shaping while the noise and interference level remains constant within the same overlapping ratio.

The average BER performance of single-PD and multi-PD reception for different power ratios of LP_{01} and LP_{11} mode with 4 users is shown in Fig. 9(a) and (b) respectively. For both single-PD and multi-PD reception, it can be seen that the maximum effective radius of the coverage for BER $\leq 3.8 \times 10^{-3}$ is increased when the power ratio is decreasing due to the high relative power of the LP_{11} mode. However, at the beam center,
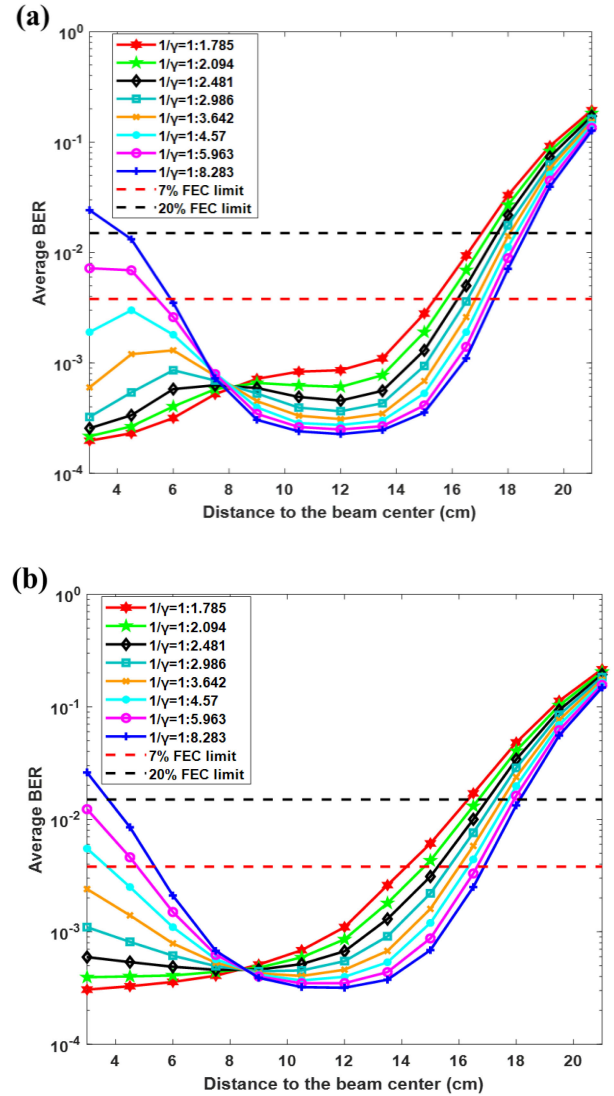
the average BER increases with the power ratio decreasing due to the lower relative power of LP_{01} mode, which results in the shrinkage of the effective coverage. Therefore, the biggest effective coverage of single-PD and multi-PD reception can be obtained with 1:3.64 and 1:4.57 of LP_{01} mode and LP_{11} mode power ratio. Similarly, when the reference BER level is set as 20% HD-FEC threshold of 1.5×10^{-2} [25], the largest effective coverage of single-PD and multi-PD reception can be obtained with 1:5.963 of LP_{01} mode and LP_{11} mode power ratio.

The aforementioned results are obtained under the assumption that the ideal synchronization can be achieved in different transmitted modes. However, in practical scenarios, different mode delay (DMD) is inevitable as they are transmitted in different paths [26], which is in contrast to the simulation shown in Fig. 2(a), where the path lengths of the transmitted LP_{01} and LP_{11} modes are considered as the same with each other because the transmitters are assumed to be ideally synchronized. In order to evaluate the impact of the DMD on the system performance,
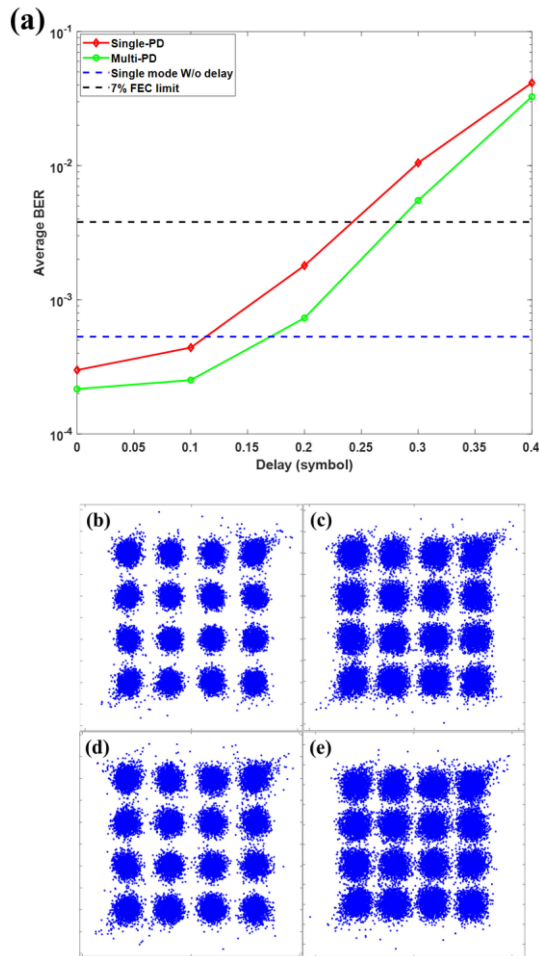
(a)

Fig. 10. (a) Average BER performance versus interval delay. (b), (d) Constellations of received signals with multi-PD and single-PD receptions at the interval delay of 0.1 symbols. (c), (e) Constellations of received signals with multi-PD and single-PD receptions the interval delay of 0.2 symbols.

we illustrate the calculated average BER performance of the received signals plotted as a function of the interval delay for the OWC system with few-mode based beam shaping incorporating non-overlapped TSC scheme which is shown in Fig. 10. It is noted that we assume the DMD mainly exists between LP_{01} and LP_{11} modes. The delay between LP_{11a} and LP_{11b} mode can be neglected as they have the same group velocity and similar transmission paths. In addition, we set interval delay caused by the MDM less than one-symbol since the delay more than one-symbol interval can be recovered by equalization and channel training, while less than 1-symbol delay is difficult to cope with as it requires precise synchronization [27]. It is worth noting that the delay interval is added onto both the modulated signals and the carrier. From Fig. 10, we can see that the tolerance to the interval delay of the single-PD and multi-PD receptions is ~0.23 and 0.28 symbols, respectively, when the error-free threshold is set as the 7% FEC limit. It can be also observed that better performance can be achieved in multi-PD and single-PD receptions when the interval delay is less than 0.1 symbols than that in single-mode transmission without interval delay. In addition, we can also conclude from

the constellation diagrams in Figs. 10(b)–(e) that the multi-PD reception outperforms single-PD reception when the interval delay is 0.1 and 0.2 symbols which is consistent with results shown in Fig. 10(a).

IV. CONCLUSION

In conclusion, we proposed a novel indoor OWC system using few-mode based beam shaping scheme to further improve the system performance for multi-user transmission with time-slot coding scheme. Through both theoretical analysis and extensive numerical simulations, it can be found that the system performance can be enhanced and the size of the effective coverage (BER$<3.8\times10^{-3}$) can be expanded to 4 times by using few-mode beam shaping, as compared to conventional OWC system without beam shaping. In addition, we have also investigated the optimal power ratios of LP_{01} mode and LP_{11} mode when achieving the maximum effective coverage under 7% and 20% HD-FEC thresholds for single-PD and multi-PD reception, when 4 users are served with gross data rate of 10Gb/s in the system. Moreover, we have found that the resistance to the code misalignment caused by imperfect timing can also be enhanced with the proposed few-mode based beam shaping and the maximum tolerance of 0.23 and 0.28 symbols to the delay interval can be achieved in single-PD and multi-PD reception, respectively.

REFERENCES

[1] D. K. Borah, A. C. Boucouvalas, C. C. Davis, S. Hranilovic, and K. Yiannopoulos, "A review of communication-oriented optical wireless systems," *EURASIP J. Wireless Commun. Netw.*, vol. 2012, no. 1, pp. 1–28, 2012.

[2] M. P. J. Lavery, H. Huang, Y. Ren, G. Xie, and A. E. Willner, "Demonstration of a 280 Gbit/s free-space space-division-multiplexing communications link utilizing plane-wave spatial multiplexing," *Opt. Lett.*, vol. 41, no. 5, pp. 851–854, 2016.

[3] O. Gonzalez, J. A. Martin-Gonzalez, M. F. Guerra-Medina, F. J. Lopez-Hernandez, and F. A. Delgado-Rajo, "Cyclic code-shift extension keying for multi-user optical wireless communications," *Electron. Lett.*, vol. 51, no. 11, pp. 847–849, 2015.

[4] H. Elgaga, R. Mesleh, and H. Hass, "Indoor optical wireless communication: Potential and state-of-the-art," *IEEE Commun. Mag*, vol. 49, no. 9, pp. 56–62, Sep. 2011.

[5] K. Wang, A. Nirmalathas, C. Lim, and E. Skafidas, "Indoor gigabit full-duplex optical wireless communication system with SCM based multiple-user access," in *Proc. IEEE Int. Topical Meeting Microw. Photon.*, 2011, pp. 45–48.

[6] T. Liang, K. Wang, C. Lim, E. Wong, T. Song, and A. Nirmalathas, "Time-slot coding scheme with adaptive loading function for multiple access in indoor optical wireless communications," *J. Lightw. Technol.*, vol. 35, no. 18, 2017, Art. no. 4079.

[7] J. Li, C. Lim, A. Nirmalathas, N. O'Keefe, and K.-L. Lee, "Demonstration of high-speed indoor optical communications using few-mode based uniform beam shaping," in *Proc. Opto-Electron. Commun. Conf.*, 2020, pp. 1–3.

[8] J. A. Hoffnagle and C. M. Jefferson, "Design and performance of a refractive optical system that converts a Gaussian to a flattop beam," *Appl. Opt.*, vol. 39, 2000, Art. no. 5488.

[9] J. Turunen, P. P. K. Nen, M. Kuittinen, P. Laakkonen, and J. Simonen, "Diffractive shaping for excimer laser beams," *J. Mod. Opt.*, vol. 47, 2000, Art. no. 2467.

[10] D. M. Brown, F. M. Dickey, and L. W. Weichman, "Multi-aperture beam integration systems," in *Laser Beam Shaping*, F. M. Dickey and S. C. Holswade, Eds. New York, NY, USA: Marcel Dekker, 2000.

[11] X. Gu, W. Mohammed, L. Qian, and P. W. E. Smith, "All-fiber laser beam shaping using a long-period grating," *IEEE Photon. Technol. Lett.*, vol. 20, no. 13, pp. 1130–1132, Jul. 2008.

[12] J. Dai and Q. Zhan, "Beam shaping with vectorial vortex beams under low numerical aperture illumination condition," in *Proc. SPIE*, 2008, Art. no. 70620D.

[13] Q. Zhan, "Properties of circularly polarized vortex beams," *Opt. Exp.*, vol. 31, no. 7, pp. 867–869, 2006.

[14] D. Zheng *et al.*, "Performance enhancement of free-space optical communications under atmospheric turbulence using modes diversity coherent receipt," *Opt. Exp.*, vol. 26, no. 22, pp. 28879–28890, 2018.

[15] C. Xu *et al.*, "All-fiber laser with flattop beam output using a few-mode fiber Bragg grating," *Opt. Lett.*, vol. 43, no. 6, pp. 1247–1250, 2018.

[16] J. Li, C. Lim, and A. Nirmalathas, "Indoor optical wireless communications using few-mode based uniform beam shaping and LMS based adaptive equalization," in *Proc. IPC*, 2020, pp. 1–2.

[17] J. M. Senior, *Optical Fiber Communications: Principles and Practice*. New York, NY, USA: Prentice Hall, 1992.

[18] X. Wang, Y. Song, F. Pang, Y. Li, and Q. Zhang, "OAM modes exchanging by controlling polarization of vortex beams propagating through an FMF-based polarization controller," *IEEE J. Quantum Electron.*, vol. 55, no. 3, pp. 1–8, Jun. 2019, Art. no. 6800308.

[19] T. Liang, K. Wang, C. Lim, E. Wong, T. Song, and A. Nirmalathas, "Time-slot coding scheme for multiple access in indoor optical wireless communications," *Opt. Lett.*, vol. 41, no. 22, pp. 5166–5169, Nov. 2016.

[20] *Safety of Laser Products*, AS/NZS 2211.1: Standards Australia International Ltd and Standards, New Zealand, 2004.

[21] P. Signal, S. Rai, R. Punia, and D. Kashyap, "Comparison of different transmitters using 1550 nm and 10000 nm in FSO communication systems," *Int. J. Comput. Sci. Inf, Technol.*, vol. 7, pp. 107–113, 2015.

[22] Z. Ghassemlooy, W. Popoola, and S. Rajbhandari, *Optical Wireless Communications: System and Channel Modelling With Matlab*. Boca Raton, FL, USA: CRC Press, 2012.

[23] Y. Wang, X. Huang, L. Tao, J. Shi, and N. Chi, "4.5-Gb/s RGB-LED based WDM visible light communication system employing CAP modulation and RLS based adaptive equalization," *Opt. Exp.*, vol. 23, 2015, Art. no. 13626.

[24] Y. Zhu, M. Jiang, and F. Zhang, "Direct detection of polarization multiplexed single sideband signals with orthogonal offset carriers," *Opt. Exp.*, vol. 26, no. 12, pp. 15887–15898, Jun. 2018.

[25] H. Ji *et al.*, "High-dimensional stokes vector direct detection over few-mode fibers," *Opt. Lett.*, vol. 44, no. 8, pp. 2065–2068, 2019.

[26] S. Randel *et al.*, "6 × 56-Gb/s mode-division multiplexed transmission over 33-km few-mode fiber enabled by 6 × 6 MIMO equalization," *Opt. Exp.*, vol. 19, no. 17, pp. 16697–16707, 2011.

[27] T. Song *et al.*, "Performance analysis of repetition-coding and space-time-block-coding as transmitter diversity schemes for indoor optical wireless communications," *J. Lightw. Technol.*, vol. 37, no. 20, 2019, Art. no. 5170.